1   **Genomic profiling reveals distinct routes to complement resistance in *Klebsiella pneumoniae***

2   Francesca L. Short,[a,b, c] Gianna Di Sario,[d] Nathalie T Reichmann,[e] Colin Kleanthous,[e] Julian Parkhill,[a, f]

3   Peter W. Taylor[d]

4

5

6

7

8

9   [a]Wellcome Sanger Institute, Wellcome Genome Campus, Hinxton, Cambridgeshire, CB10 1SA, UK

10   [b]Department of Medicine, University of Cambridge, Addenbrookes Hospital, Hills Road, Cambridge

11   CB2 0QQ, UK

12   [c]Present address: Department of Molecular Sciences, Macquarie University, NSW 2109, Australia

13   [d]School of Pharmacy, University College London, 29-39 Brunswick Square, London, WC1N 1AX

14   UK

15   [e]Department of Biochemistry, University of Oxford, University of Oxford, South Parks Rd, Oxford,

16   OX1 3QU, UK

17   [f]Department of Veterinary Medicine, University of Cambridge, Madingley Road, Cambridge,

18   CB3 0ES, UK

19   Address correspondence to: Francesca Short, fs13@sanger.ac.uk , francesca.short@mq.edu.au

20 **ABSTRACT**

21 The serum complement (C') system is a first line of defense against bacterial invaders. Resistance to

22 killing by serum enhances the capacity of *Klebsiella pneumoniae* to cause infection, but is an

23 incompletely understood virulence trait. Identifying and characterising the factors responsible for

24 preventing activation of, and killing by, serum C' could inform new approaches to treatment of *K.*

25 *pneumoniae* infections. We have used functional genomic profiling to define the genetic basis of C'

26 resistance in four diverse serum-resistant *K. pneumoniae* strains (NTUH-K2044, B5055, ATCC43816

27 and RH201207), and explored their recognition by key complement components. Over 90 genes

28 contributed to resistance in one or more strains, but only three, *rfaH*, *lpp* and *arnD*, were common

29 to all four. Deletion of the anti-terminator *rfaH*, controlling expression of capsule and O-side chains,

30 resulted in dramatic C' resistance reductions in all strains. The murein lipoprotein gene *lpp* promoted

31 capsule retention through a mechanism dependent on its C-terminal lysine residue; its deletion led

32 to modest reductions in C' resistance. Binding experiments with the C' components C3b and C5b-9

33 showed that the underlying mechanism of evasion varied in the four strains: B5055 and NTUH-K2044

34 appeared to bypass recognition by C' entirely, while ATCC43816 and RH201207 were able to resist

35 killing despite being associated with substantial levels of C5b-9. All *rfaH* and *lpp* mutants bound C3b

36 and C5b-9 in large quantities. Our findings show that, even amongst this small selection of isolates,

37 *K. pneumoniae* adopts differing mechanisms and utilises distinct gene sets to avoid C' attack.

38

39 **INTRODUCTION**

40 The opportunistic pathogen *Klebsiella pneumoniae* is a major public health threat due to its

41 propensity to become extensively drug resistant (1, 2), the emergence of hypervirulent strains (3–5),

42 and the recent evolution and increasing prevalence of strains displaying both hypervirulence and

43 extensive drug resistance (6, 7). Virulence in *K. pneumoniae* is multifactorial and depends on both

44 core-encoded and horizontally-acquired factors (8, 9). Capsule is a critical *K. pneumoniae* virulence

45 determinant present in all clinical strains; mutants lacking capsule are avirulent, whilst

46 overproduction of capsule is associated with hypervirulent strains and more severe disease in animal

47 models (10, 11). Over 130 capsule locus types have been described in *K. pneumoniae* (12), and

48 hypervirulent strains usually produce capsule type K1 or, less frequently, K2. Nine lipopolysaccharide

49 (LPS) O side chain groups have been identified and characterized in *K. pneumoniae* (13); these

50 moieties modulate innate immune signalling and may contribute towards serum resistance.

51 Horizontally-acquired virulence genes include siderophores and capsule up-regulators (9, 14). In

52 general, understanding *K. pneumoniae* pathogenesis is confounded by the phylogenetic breadth of

53 infectious lineages, and by the diversity of the virulence factors themselves.

54 The complement (C') system, comprising more than twenty proteins in serum and tissue fluids, is a

55 first line of defense against bacterial invaders that have breached the host's epithelial barriers.

56 Resistance to C' is strongly correlated with the capacity for systemic survival, multiplication and

57 spread of a wide range of Gram-negative pathogens (15), and is a major virulence trait enabling *K.*

58 *pneumoniae* to elicit invasive infections (16, 17). The C' cascade can be activated via the classical,

59 alternative and lectin pathways, which each act in a precise sequence of reactions to facilitate C3b

60 deposition on to the target bacterial surface. The classical pathway is initiated following recognition

61 of antigen-antibody complexes on the bacterial cell surface by hexameric C1q, whereas the lectin

62 pathway begins with detection of bacterial surfaces by pattern recognition molecules such as

63 mannose-binding lectin or the ficolins (15, 18, 19). All pathways converge at C3 cleavage with the

64 larger cleavage product C3b covalently bound to the target surface. Accumulation of anchored C3b

65   by amplification leads to the assembly of C5 convertases that generate the C5b cleavage product

66   which spontaneously associates with one molecule each of C6, C7, C8 and multiple copies of C9 to

67   form the C5b-9 membrane attack complex. In C' susceptible bacteria, C5b-9 complexes intercalate

68   into the outer membrane (OM) bilayer and perturb the cytoplasmic membrane through an

69   incompletely defined process (20–22).

70   Gram-negative bacterial resistance to C' can be due to failure of activation of any of the C' pathways,

71   degradation of activated C' proteins, arrest of activated pathways by C' inhibitors such as C1-

72   inhibitor protein (C1-Inh), factor H (fH) and C4 binding protein (C4bp), or the inability of C5b-9

73   complexes to assemble and insert into the OM (which can be a result of impedance by bacterial

74   surface structures)(15). The basis of the C' resistance of *K. pneumoniae* is still poorly understood.

75   Though it has been reported that limiting C' activation and C3b accumulation is the primary mode of

76   resistance, both C' resistant and susceptible clinical isolates and mutants may activate C' cascades

77   after exposure to human serum (23–26) . Multiple different factors can influence serum resistance in

78   *K. pneumoniae* including capsule type and amount, O-antigen type, and various surface proteins;

79   capsules and O-antigens have each been invoked as the main determinant of C' resistance (9, 27).

80   However, a recent study of >150 *K. pneumoniae* clinical isolates from Thailand of varying C'

81   susceptibility concluded that susceptibility did not correlate with the presence of specific genes,

82   particular capsule types, or even with the hyper-capsulation phenotype of the isolates (28). This

83   study highlighted the main limitation of collective studies on C' resistance in *K. pneumoniae* to date -

84   that although many resistance factors are individually well-characterised, there is very limited

85   understanding of how their activities play out in different combinations, or across diverse isolates of

86   *K. pneumoniae*.

87   Untangling the mechanisms behind C' resistance in *K. pneumoniae* will lead to better understanding

88   of the virulence of this bacterium and will provide avenues to target C' resistance in the clinic,

89   particularly in view of growing interest in the targeting of capsule and other virulence factors as an

90   anti-infective strategy for *K. pneumoniae* (29–31). In particular, developing generally applicable

91   (rather than K type-specific) therapeutics that promote C' killing requires deeper knowledge of the

92   activity of different C' resistance factors in diverse strains. In this study we used functional genomic

93   profiling by transposon-directed insertion site sequencing (TraDIS) to define the genetic basis of

94   serum survival in four diverse strains of *K. pneumoniae*. We show that C' resistance is multifactorial

95   and strain-specific, and identify RfaH and Lpp as shared *K. pneumoniae* resistance determinants. Two

96   of the strains evaded C' evasion by preventing C3b and C5b-9 accumulation at the cell surface, which

97   was disrupted in Δ*rfaH* and Δ*lpp* mutants, whilst the remaining two strains were resistant to serum

98   despite substantial C5b-9 deposition. Our results present a picture of at least two distinct modes of

99   C' resistance in *K. pneumoniae* and point to RfaH and Lpp as potential targets for C'-sensitizing

100   therapeutics.

101

102   **RESULTS**

103   **Serum resistant isolates of *K. pneumoniae*.** Three well-studied hypervirulent *K. pneumoniae* strains

104   and one recently-isolated classical strain were tested for survival in human serum (Table S1, Fig. 1A).

105   B5055 (sequence type ST66) produces a type K2 capsule, and was originally isolated from a sputum

106   sample in the 1920s.   NTUH-K2044 is a hypervirulent strain (sequence type 23) producing a K1

107   capsule, and was the first characterized liver abscess-causing *K. pneumoniae* isolate (32). ATCC43816

108   is another K2 strain commonly used in mouse virulence studies (33). *K. pneumoniae* RH201207 is a

109   colistin-resistant ST258 strain obtained from Public Health England in 2012 (34). These strains differ

110   in their capsule production as determined by uronic acid assay, with B5055 and NTUH-K2044

111   producing copious capsule and ATCC43816 and RH201207 producing less (Fig. 1B). All four strains

112   survived exposure to 66% normal human serum (a potent source of C') over a 3 h incubation period

113   at 37 ^{o}C when an inoculum of 1 x 10^6 was employed (Fig. 1C); strains B5055, NTUH-K2044 and

114   ATCC43816 proliferated in serum whereas viable counts for RH201207 did not change between 0-2 h

115   but showed a slight reduction at 3 h. A sensitive control strain, *Escherichia coli* DH5α, showed no

116   viability after 30 min incubation and killing of all strains was completely abrogated by heat

117   inactivation (56 °C, 30 min; data not shown).

118   **TraDIS analysis of C' resistance in *K. pneumoniae* isolates.** We performed transposon-insertion

119   sequencing of saturated mutant libraries exposed to serum to define the genes contributing to

120   serum survival in each of the four *K. pneumoniae* strains. The *K. pneumoniae* B5055 library was

121   constructed for this study by conjugative delivery of pDS1028 and contained 225,000 unique

122   transposon insertions (see Materials and Methods; Table S2), while NTUH-K2044, ATCC43816 and

123   RH201207 mutant library construction has been previously described (34, 35). Our experimental

124   strategy was similar to that used in previous work with *E. coli* ST131 (36), with libraries treated with

125   either normal human serum or heat-inactivated serum for 90 min, outgrown for 2 hours, and

126   sequenced and mapped using the BioTraDIS pipeline (37). Putative serum resistance genes were

127   defined as those with altered mutant abundance in the serum-treated libraries in comparison to the

128   control libraries treated with heat-inactivated serum (log2-fold change of < -1 or > 1 NS vs HI-S, q-

129   value of <0.005; Table S3). Comparing to the heat-inactivated serum control, rather than the input

130   library, minimises the chance of spurious hits to mutants with general growth defects.

131   A total of 93 genes were identified that altered serum survival in one or more *K. pneumoniae* strains

132   (Fig. 2; Table S4), with the number of hits in each strain ranging from 22 (for B5055) to 54 (for

133   RH201207). These genes included 43 core or soft-core *K. pneumoniae* genes (present in >99% or 95-

134   99% of *K. pneumoniae* strains), 24 shell genes (15-95% strains) and 26 cloud genes (<15% strains).

135   Despite the high proportion of shell and cloud genes, 60 of the serum survival-related genes were

136   present in all four of the strains examined. Putative serum resistance genes came from multiple

137   functional categories including synthesis of surface polysaccharides, metabolism, cell surface or

138   membrane structure and function, and transcriptional regulation (Fig. 3; Table S4). Overall, there

139   was an unexpected strain specificity in the exact genes identified: even among the 60 hit genes

140   present in all four strains, the majority (35 genes) influenced serum survival in only one strain, 22

141   genes were hits in two or three strains, and only three genes affected serum survival in all four *K.*

142   *pneumoniae* (Fig. 2A; Fig. 3).

143   **Contribution of capsule to serum resistance.** Capsule biosynthetic genes (*cps*) were among the

144   putative serum survival factors in the four strains investigated. The proportion of *cps* locus genes

145   contributing to C' resistance and the magnitude of the fitness changes involved varied between

146   isolates (Fig. 2B, Fig. 3). Note that mutagenesis of genes of the capsule locus can cause secondary

147   cell envelope defects (shown for *wza* and *wzi* (38)), and not all *cps* locus mutations entirely eliminate

148   capsule production (35, 39); therefore complete consistency of selection across all genes of the *cps*

149   locus is not expected. With *K. pneumoniae* B5055, which produces copious amounts of K2 capsule,

150   11/18 genes of the *cps* locus were called as hits, accounting for half of the serum survival

151   determinants of this strain. They included the exporter *wzi*, the sugar precursor genes *manBC*, *galF*

152   and the majority of K-type specific genes in the central operon of the K2 locus (Fig. 3; Fig. S1). The

153   majority of these genes were also required in the K2 strain ATCC43816 (Fig. 3; Fig. S1), with the

154   exceptions of *wzi*, and the sugar precursor genes *manB* and *ugd* (which had too few reads in this

155   strain for serum-specific effects to be measured). In NTUH-K2044, 8/20 *cps* genes were called as hits

156   and in RH201207 this proportion was 9/19 (Fig. 3; Fig. S1). Because the pDS1028 transposon has

157   transcriptional read-out from one end, transposon insertions are not predicted to dramatically

158   disrupt downstream gene expression in the NTUH-K2044, B5055 and ATCC43816 libraries. This effect

159   is clear in NTUH-K2044, where transposon insertions in several genes of the *cps* locus

160   (*magA*/KP1_3714, *wzc*, *wzb*, *wza*/KP1_3718:KP1_2730, none of which were defined as serum-

161   related) are counter-selected by serum on one strand but unaffected on the other (Fig. S1). The

162   RH201207 library was constructed using a different transposon, and transcriptional read-through is

163   not expected in this library. Our TraDIS results indicate that all *K. pneumoniae* strains require capsule

164   to some extent to withstand serum challenge. Known regulators of capsule biosynthesis also

165   influenced serum survival, including the anti-terminator gene *rfaH* in all four isolates (40, 41), *rmpC*

166   (BN49_pII0025) in B5055 only (42), and *rcsB* in RH201207 (43). We hypothesise that *rcsB* mutant

167 showed a serum survival defect only in the RH201207 background because this strain produces less

168 capsule than the other three strains, making it more sensitive to mutations that further reduce

169 capsule expression. Mutation of the *rmpC* gene had no effect in NTUH-K2044; however, this strain

170 encodes both chromosomal and plasmid copies of *rmpC*.

171 **Contribution of LPS O-side chains to serum resistance.** Enterobacteriaceae lacking LPS O-side chains

172 are generally susceptible to C5b-9-mediated killing (44) and introduction of genes determining O-

173 side chains into a highly C'-sensitive rough *E. coli* strain elicited a large increase in C' resistance (45).

174 With our four *K. pneumoniae*, the majority of O-antigen genes showed a serum fitness defect when

175 mutated (Fig. 2B; Fig. 3), with the exception of those of *K. pneumoniae* B5055. This is surprising

176 because B5055 encodes the same O-antigen type (O1v1) as NTUH-K2044, in which O-antigen

177 mutants showed a drastic fitness defect (Fig. 2B; Fig. 3). We suggest that the B5055 strain is almost

178 completely protected from serum bactericidal activity by its thick K2 capsule, masking the additional

179 protective activity of the O-antigen. *K. pneumoniae* ATCC43816 produces K2 capsule, albeit in lower

180 amounts than B5055, but still required O-antigen for serum survival. These findings suggest that the

181 K2 capsule is sufficient to completely protect from C'-mediated killing when produced in copious

182 amounts, whilst K1 capsule is not, at least in these isolates.

183 LPS core biosynthetic genes contributed to serum fitness in isolates ATCC43816 and NTUH-K2044

184 (Table S4), although the same genes were either essential or had no effect on resistance in B5055,

185 and were also not identified as statistically significant hits in RH201207. Note that mutation of many

186 LPS core genes causes a severe general fitness defect, so their specific contributions to serum

187 resistance are not always easy to define. A small subset of the genes (*arnD-arnF*) in the *arn/pmr*

188 operon responsible for LPS lipid A modification showed C' resistance defects in one or more strains

189 when mutated (Fig. 2B). This was unexpected as the L-Ara4N lipid A modification is rarely made *in*

190 *vitro*, and is not produced in rich media conditions as used in this study (46). Loss of any of the

191 *arnDEF* genes was previously shown to reduce *K. pneumoniae* mucoviscosity in a genome-wide

192   density-based screen (35), and we suggest that reduced capsule production underpins the serum

193   survival defects seen here.

194   **Other genes implicated in serum survival.** Mutation of several genes involved in cell membrane or

195   cell wall structure and function resulted in fitness defects in serum. These genes included *dacA*

196   (RH201207 only) involved in cell wall biosynthesis, the inner membrane protein *dedA* (in isolates

197   B5055, NTUH-K2044 and ATCC43816) which has a role in membrane integrity, and components of

198   the *tol-pal* outer membrane transporter (NTUH-K2044 and ATCC43816). Finally, the outer

199   membrane lipoprotein Lpp was required for full serum resistance in all four strains. A number of

200   metabolic genes were also implicated in serum survival, primarily those involved in pyrimidine

201   metabolism, and metabolism of carbohydrates (Fig. 3; Table S4). Some of these genes (*pgi*, *pgm*) are

202   involved in precursor molecule biosynthesis for capsule and LPS.

203   **Increased serum survival genes in *K. pneumoniae* RH201207.** Five genes of *K. pneumoniae*

204   RH201207, *csrD*, *fabR*, *wecB*, *wecC* and *cyoA*, led to increased serum fitness when mutated. CsrD

205   promotes degradation of the capsule-regulating small RNA CsrB; mutation of *csrD* can promote

206   capsule production (as measured by density) (35), which may explain the enhanced serum survival of

207   this mutant. FabR, WecB and WecC are not predicted to affect capsule, but all three genes have

208   roles relating to the cell envelope: FabR is a transcriptional regulator which controls the ratio of

209   saturated to unsaturated fatty acids in the cell membrane, and WecB and WecC produce the second

210   component of enterobacterial common antigen (*N*-acetyl-D-mannosaminuronic acid) and attach this

211   to UDP-GlcNac. We speculate that loss of *wecB* and *wecC* increases the pool of UDP-GlcNac in the

212   cell, which is then diverted into O-antigen biosynthesis (which also utilise UDP-GlcNac) (47). The

213   cytochrome ubiquinol oxidase component CyoA also resulted in increased serum survival when

214   mutated through an unknown mechanism. The identification of mutants with increased serum

215   fitness in RH201207, but not the other *K. pneumoniae* strains, is consistent with the observation that

216   serum survival of *K. pneumoniae* RH201207 is less dependent on capsule.

217 **Confirmation of RfaH and Lpp as shared serum resistance factors in *K. pneumoniae* isolates.** Only

218 three genes affected serum survival in all four strains tested: the LPS modification gene *arnD*, the

219 outer membrane lipoprotein *lpp*, and the transcription anti-terminator *rfaH* (Fig. 2; Fig. 3). We

220 selected Lpp and RfaH for further characterisation as potential core serum resistance factors of *K.*

221 *pneumoniae*. ArnD was not selected for follow-up because we failed to detect the relevant LPS

222 modification *in vitro* (which is consistent with previous reports that the modification is made *in vitro*

223 only under very specific conditions (46)) and therefore presumed its activity was indirect, though the

224 potential role of lipid A modifications in *K. pneumoniae* C' resistance may be of interest for a future

225 study. Deletion mutants of *rfaH* and *lpp* were constructed in *K. pneumoniae* NTUH-K2044, B5055 and

226 ATCC43816 by allelic exchange. In isolate RH201207, an insertion mutant in *rfaH* was obtained but a

227 *Δlpp* mutant could not be generated despite multiple attempts. Serum survival assays were

228 conducted with an inoculum of 10^6 cells in 66% normal human serum and bacterial counts

229 monitored for 3 h (Fig. 4). Loss of *rfaH* caused a large reduction in serum survival in all four strains,

230 and complementation of with plasmid-encoded *rfaH* expressed from its native promoter restored

231 wild-type survival, confirming the importance of RfaH in C' resistance (Fig 4). Loss of *lpp* caused a

232 modest change in C' sensitivity (Fig 4); these mutants lost the ability to proliferate in serum (note

233 that *lpp* disruption does not cause a general growth defect, Fig S2B and Table S3), and with NTUH-

234 K2044 *Δlpp* delayed C' killing was observed. The *Δlpp* mutations could not be complemented by

235 expression of *lpp* from its native promoter due to unexpected toxicity during cloning. Expression of

236 *lpp* from an arabinose-inducible promoter also failed to complement the serum proliferation defect

237 of the *Δlpp* mutants. We suspect that this was due to insufficient expression. In addition,

238 proliferation of the vector-only control strains was impaired by addition of arabinose (data not

239 shown). Though we were unable to find an appropriate system for complementation of the *Δlpp*

240 mutants, their phenotypes align with the results of the genome-scale screens (Fig 2, Fig 3), as well as

241 published work on Lpp in *K. pneumoniae* NTUH-K2044 (48).

242   We were intrigued by the variable requirement for different genes of the *cps* locus seen in TraDIS,

243   and several randomly-isolated capsule locus mutants of ATCC43816 and RH201207 were also

244   examined for serum survival in order to further validate the genome-scale screens (Fig S2). Each of

245   these mutants showed the phenotype predicted based on TraDIS screening: ATCC43816 i-*wcaJ*,

246   which was not identified as a serum resistance gene, multiplied to the same extent as wild type,

247   ATCC43816 i-*wza* did not proliferate in serum, and RH201207 i-*wzc* was rapidly susceptible.

248   RH201207 i-*wcaJ*, which was not a hit, was viable after 90 minutes (our TraDIS timepoint), but

249   showed a delayed susceptibility to serum. Note that *wcaJ* deletion in *K. pneumoniae* does not

250   completely eliminate K2 capsule production, and can also have pleiotrophic effects including

251   rounded cell morphology and increased fitness under nutrient limitation (38, 39) – therefore, the full

252   resistance of ATCC43816 i-*wcaJ* does not preclude a role for capsule in the C' resistance of this

253   strain. Taken together, the results of serum survival assays with defined mutants show perfect

254   agreement with the phenotypes predicted from TraDIS screens (for 11/11 mutants), and establish

255   RfaH and Lpp as shared serum resistance factors in *K. pneumoniae*. These experiments also revealed

256   additional subtleties in the serum resistance phenotypes of the mutants, with survival patterns

257   roughly following the underlying resistance of the parent strain (for example, ATCC43816 Δ*rfaH* and

258   RH201207 Δ*rfaH*), and some differences only revealed at later stages of incubation (eg. RH201207 i-

259   *wcaJ*).

260   **Lpp influences capsule retention but not capsule production and requires lysine-78.** The

261   antiterminator RfaH and the murein lipoprotein Lpp contributed to C' resistance in all four *K.*

262   *pneumoniae* strains. Lpp is an extremely abundant protein which contributes to cell envelope

263   integrity by connecting peptidoglycan to the cell outer membrane (48, 49). We observed that the

264   Δ*lpp* mutant colonies were flat and unstructured in comparison to wildtype, although their opacity

265   suggested they still produced capsule. To examine the effect of the *lpp* mutation further we

266   measured total and cell-attached capsule using the uronic acid assay. All three *K. pneumoniae* Δ*lpp*

267   mutants produced capsule at wildtype levels, but showed moderate decreases in amounts of cell-

268 associated capsule (Fig 5A). Mutants of *rfaH* showed dramatically reduced capsule amounts (Fig 5B).

269 We then tested whether Lpp activity requires covalent linkage to peptidoglycan, mediated through

270 the ε-amino group of the C-terminal lysine residue in Lpp and the meso-diaminopimelic acid residue

271 on the peptidoglycan peptide stem (50). Expression of Lpp from an arabinose-inducible vector

272 partially complemented the hypermucoid phenotype of NTUH-K2044 and B5055 (Fig 5C). Partial

273 complementation was not seen with an Lpp-ΔK78 construct, confirming that the C-terminal lysine is

274 required in order for Lpp to promote capsule retention in both K1 and K2 strains. The shared serum

275 survival factors Lpp and RfaH therefore both appear to function at least partly through effects on

276 capsule.

277 **Deposition of C3b and C5b-9 complexes.** Genome-scale screening revealed a very high degree of

278 strain specificity in the serum resistance determinants across four *K. pneumoniae* strains. We

279 decided to explore complement activation by these strains, and how this is affected by loss of *rfaH*

280 or *lpp*. Activation of any or all C' pathways will lead to C3b generation and binding to the target

281 bacterial surface; subsequent formation of C5 convertase complexes may lead to deposition of

282 membrane attack complexes and cell death (15, 19). Surface C3b deposition and C5b-9 formation on

283 *K. pneumoniae* strains and mutants during incubation with human serum are reported in Figs 6 7, S3

284 and S4. Unlike the three hypervirulent strains that showed little to no C3b binding, serum exposure

285 of RH201207 led to a considerable increase in levels of C3b and C5b-9 over time (Fig 6A, 7A, S3, S4A).

286 ATCC43816 also showed C5b-9 binding at later time points, while B5055 and NTUH-K2044 did not. In

287 all backgrounds, the deletion of *rfaH* led to significant levels of C3b and C5b-9 binding compared to

288 wild type, with a peak after 2-3 hours of serum exposure (Fig 6A and 7A), confirming that the

289 mechanism of serum killing observed (Fig 4) is through formation of the membrane attack complex.

290 With B5055Δ*rfaH*, cells could not be examined beyond the 30 min time point due to cell lysis as

291 determined by the release of cytoplasmic GFP from strain B5055 Δ*rfaH* pFLS21 (Fig S4B). Imaging of

292 the Δ*rfaH* mutants showed that C3b binding is evenly distributed over the cell surface and occurs

293 within 5 min of serum exposure (Fig 6B), whilst C5-9 deposition is minimal at 5 min (except for

294 ATCC43816) and uniformly detected at 15 min (Fig 7B). Similarly, Δ*lpp* mutants were also found to

295 significantly bind C3b and C5b-9 compared to wild type, though to a lesser extent than the Δ*rfaH*

296 mutants (Fig 6A, 7A, S3 and S4). Most Δ*lpp* mutant cells maintained their rod-shape following 15min

297 of serum exposure (Fig 6C, 7C) which correlates with increased serum susceptibility only after longer

298 exposure times (Fig 4). By examining cell population dynamics we observed that Δ*lpp* mutants

299 showed a similar distribution to wild type cells (Fig S3 and S4A, third columns). In contrast, Δ*rfaH*

300 mutants displayed a more compact distribution in Q2 quadrant, suggesting that not only do more

301 Δ*rfaH* cells bind C3b and C5b-9 over time, but that the level of binding to individual cells increases.

302 These findings indicate that B5055, NTUH-K2044, ATCC43816 and RH201207 activate the

303 complement system to different extents, and that loss of *lpp* or *rfaH* increases the recruitment of

304 complement components.

305

306 **DISCUSSION**

307 Resistance to killing by C' is an important yet incompletely understood feature of *K. pneumoniae*

308 pathogenesis (4, 8, 28). The prominent polysaccharide capsule has been invoked as a key

309 determinant of resistance by virtue of its capacity to limit C3b deposition or assembly of the

310 membrane attack complex (8, 27) but it is clear that other factors also contribute to the C' resistant

311 phenotype (28). Resistance to serum killing is associated with *K. pneumoniae* hypervirulence and we

312 therefore selected three well-studied hypervirulent strains as well as a recently-isolated clinical

313 strain for our analyses. To our knowledge, this study represents the first multi-strain functional

314 genomics study of C' resistance in any bacterial species.

315 TraDIS identified 93 genes that impacted serum survival in one or more strains but only three of

316 these, *rfaH*, *lpp* and *arnD*, were common to all four strains. All three genes influence the physical

317 characteristics of the outer surface of *K. pneumoniae*. RfaH controls transcription of operons that

318 direct synthesis, assembly and export of the lipopolysaccharide core and capsular polysaccharide in

319 *E. coli* and other gram-negative bacteria (41), the abundant peptidoglycan-linked outer membrane

320   protein Lpp is involved in the maintenance of cell envelope integrity and retention of capsule at the

321   cell surface (Fig 5A)(35, 50), and the *arn* operon encodes proteins that participate in the addition of

322   4-amino-4-deoxy-L-arabinose to lipid A (51) and may also affect capsule levels through an unknown

323   mechanism (35). Deletion of *rfaH* markedly increased C' susceptibility in all four strains, confirming

324   the key contributions of capsule and LPS O-side chains to the resistant phenotype. However, there

325   were strain differences in the rate of C' killing; *K. pneumoniae* RH201207Δ*rfaH* was rapidly killed,

326   while ATCC43816 and NTUH-K2044 displayed a delayed killing response typical of smooth (O-side

327   chain-replete) C' susceptible Gram-negative bacteria (52). RH201207 possesses LPS O-side chains but

328   elaborates less capsule than the other three. These C' susceptibility profiles emphasize the

329   interdependence of the various surface structures that contribute to serum resistance. Deletion of

330   *lpp* in the three hypervirulent isolates modified the serum responses but to a variable degree: the

331   loss of proliferation in serum of strains ATCC43816 and B5055 was not sufficient to convert them to

332   full C' susceptibility whereas the degree of C' killing of *K. pneumoniae* NTUH-K2044Δ*lpp* was more

333   pronounced. Although capsule retention is impaired in the *lpp* mutants, reducing the protective

334   barrier against C' binding, the presence of large amounts of unattached polysaccharide is likely to

335   have caused off-target C' activation (26) and depletion of C' components in the serum, resulting in

336   less pronounced killing than *rfaH* mutants.

337   Removal of the capsule by deletion of *rfaH* (Fig 5B) led to significant deposition of C3b on the outer

338   surface in all four strain backgrounds. Deletion of *rfaH* presumably caused loss of O-side chains as

339   well as capsule, as shown in *E coli* and other gram-negative bacteria including *Salmonella enterica*

340   and *Yersinia enterocolitica* (41, 53, 54). The formation of C5b-9 complexes at the cell surface and

341   subsequent changes in cell morphology point to a loss in integrity of both the outer membrane and

342   peptidoglycan layer, eventually leading to cell lysis, though the exact mechanism by which the inner

343   membrane is disrupted is not yet understood. With the Δ*lpp* mutants, which have detached capsule

344   (Fig 5) and increased membrane permeability but retain their O-antigen (48), sufficient deposition of

345   C3b and perturbation of the cell envelope by C5b-9 complexes occurred to prevent proliferation in

346   serum as seen in Fig. 4. While B5055 and NTUH-K2044 did not show detectable C3b or C5b-9 levels

347   by flow cytometry, the C' resistant ATCC43816 showed a limited increase in levels of C5b-9

348   complexes following serum exposure, despite these not functioning as bactericidal entities (Figs 6A

349   & 7A; Fig. S4A). Finally, although the classical isolate RH201207 survived 2-3 h serum incubation,

350   both C3b and C5b-9 levels rose dramatically following incubation with serum.

351   These differences in the interplay between surface factors and the C' system are unlikely to be due

352   to differences in strain-to-strain gene content. Around half of the hit genes were present in all four

353   strains but contributed to complement resistance in only one or two (46 of 93 total genes, 60 of

354   which were present in all strains), and this trend held when the classical RH201207 strain was

355   excluded (of 36 hits in B5055-NTUH-K2044-ATCC43816 shared genes, 12 were specific to one strain,

356   19 were hits in two strains and only 5 were hits in 3 strains). However, the degree of strain specificity

357   we found is broadly comparable to that observed for daptomycin resistance genes in two strains of

358   *Streptococcus pneumoniae*, which showed only 50% overlap despite the two strains sharing 85% of

359   their genes (55). Furthermore, bacteria such as *Salmonella* spp, *Mycobacterium tuberculosis* and

360   *Pseudomonas aeruginosa* have been shown to possess strain-specific essential gene sets by

361   TraDIS/TnSeq methods (56–58).

362   Strain specific effects are likely to be due to a combination of imperfect hit identification, functional

363   divergence of genes in different strains, and context-dependent fitness contributions of genes with

364   the same activity, due to either redundancy with other factors or differences in the relative

365   contribution of each gene to overall bacterial surface architecture. For example, the O1v2-type O-

366   antigen produced by both NTUH-K2044 and B5055 contributed to serum resistance only in the

367   former strain, presumably because in B5055 the protection from the capsule is so strong that other

368   factors are not needed. We speculate that such context-dependent fitness effects may be a common

369   feature in bacterial populations. Our finding that vastly different gene sets underpin serum survival

370   in four strains support the notion that serum resistance is determined by the overall biophysical

371   properties of the cell surface, rather than any single factor, and also show that there are multiple

372   routes by which a C'-resistant cell surface can be generated.

373   A limitation of our study is that *K. pneumoniae* is a highly genetically diverse species (59), and the

374   four isolates that we studied do not cover the range of potential combinations of cell surface

375   structures that may impact survival in serum. We did note that the classical strain RH201207 was

376   markedly different from the three hypervirulent strains in terms of genes involved in C' resistance

377   and C' binding patterns; it would be useful to explore the properties of other classical strains in

378   future studies. Another limitation is that in order to maintain library diversity and provide enough

379   material for sequencing we based our TraDIS strategy on that used by Phan and co-workers (36),

380   employing a library inoculum of 10^8 CFU with only a single 90 min time point, which may have

381   missed delayed or subtle effects on C' resistance. Though high-throughput mutagenesis studies such

382   as ours are the only way to profile the contributions of all non-essential genes to serum survival,

383   mutation or deletion of genes encoding major surface structures (such as capsule, LPS O-side chains

384   and abundant membrane proteins) may force a major reconfiguration of the cell surface as a

385   compensatory mechanism to deal with envelope stress (60); conversion of C'-resistant cells to C'-

386   susceptible could be a consequence of this compensatory response as well as loss of the structure

387   itself. In particular, capsule locus mutations can have a range of secondary effects including changes

388   to cell envelope integrity, cell morphology and growth rate, and some do not fully abolish capsule

389   production (38, 39). Such effects cannot be detected or avoided by employing different mutagenesis

390   strategies (eg. gene deletion vs transposon insertion) or by complementation. While these findings

391   fit with the range of serum resistance phenotypes we observed among different *cps* locus mutants

392   (Fig S1 and Fig S2A), they also suggest that any data derived from capsule mutant strains should be

393   interpreted with caution. More direct information comes from recent studies using phage-derived

394   capsule depolymerases, where *K. pneumoniae* strains are stripped of capsule prior to treatment with

395   serum. In this way, at least eight different capsular types of *K. pneumoniae* have been confirmed to

396   protect from serum to date, including type K1 (of NTUH-K2044) (61–66). The magnitude of the

397   change in serum sensitivity following enzymatic capsule removal varies depending on both the strain

398   and the capsule type. We are currently examining the impact of capsule removal on complement

399   susceptibility in systematic fashion using enzymes selective for the most frequently isolated *K.*

400   *pneumoniae* capsular serotypes. Despite its inherent limitations, our genome-scale screening gives a

401   picture consistent with recent phage depolymerase work and the collective molecular

402   microbiological studies (9, 27)– *K. pneumoniae* capsule can protect from serum killing, and the

403   strength of this protection depends on capsule type, capsule thickness and the strain background.

404   The data suggest that *K. pneumoniae* may adopt different strategies for evasion of C'-mediated

405   attack. Isolates may fail to strongly activate C' pathways (B5055; NTUH-K2044) or activate one or

406   more pathways but avoid C5b-9-mediated lethality (ATCC43816). With either scenario the capsule is

407   likely to be critical. Implicit in the design of bactericidal assays is the assumption that normal human

408   serum contains IgM or IgG subclasses directed against exposed bacterial surface antigens with the

409   capacity to efficiently activate the classical pathway (67); this is certainly the case with much-studied

410   *E. coli* strains but less clear with *K. pneumoniae*. After activation, C5b-9 will engender lethal

411   membrane damage only after disruption of lipid domains on the bacterial surface, resulting in a

412   drastic change to membrane topology and architecture. C' resistant bacteria may not only mask their

413   cell surface from the initial recognition by the three C' pathways, but also inhibit later stages of the

414   C' pathway by altering their surface configuration in response to envelope stress and preventing

415   membrane insertion and MAC pore formation. Our findings that distinct *K. pneumoniae* strains can

416   have distinct C' evasion mechanisms, underpinned by dramatically different gene sets, highlights the

417   complexity associated with predicting serum resistance based on genome sequence or single

418   virulence factors – an undertaking which is not yet possible for *K. pneumoniae* (28). A

419   comprehensive understanding of the basis of C'-resistance in Gram-negative bacteria will only be

420   forthcoming when the behavior of such clinically relevant pathogens can be explained.

421

422   **MATERIALS AND METHODS**

423 **Construction of the *K. pneumoniae* B5055 TraDIS library.** The *K. pneumoniae* B5055 transposon

424 mutant library was constructed by conjugation with *E. coli* β2163 pDS1028 as described (35), with

425 selection of transposon-containing *K. pneumoniae* B5055 colonies performed at 25 ˚C on LB agar

426 supplemented with 25 µg/ml chloramphenicol. Approximately 600,000 colonies were scraped,

427 pooled and used as the final B5055 TraDIS library.

428 **Serum challenge of TraDIS libraries.** Experiments were performed in biological triplicate. TraDIS

429 libraries were grown overnight in 10 ml LB with an inoculum of 10-20 µl, which was sufficient to

430 ensure representation of the entire mutant library. Overnight cultures were diluted 1:25,

431 subcultured in 25 ml LB in a 250 ml flask, and grown 37°C at 180 rpm on an orbital incubator to OD_{600}

432 of 1. A 1ml aliquot of each culture was centrifuged for two min at 8000 g and resuspended in sterile

433 PBS. 500 µl of bacterial suspension was added to 500 µl normal human serum (Sigma, S7023) and

434 incubated at 37°C for 90 min. Control reactions were performed in the same way, except that serum

435 was heat-inactivated at 56°C for 30 min prior to use. Following incubation, serum reactions were

436 centrifuged, the pellets suspended in 10 ml LB and the surviving bacteria outgrown at 37°C for 2 h.

437 **DNA extraction and next-generation sequencing.** Genomic DNA (gDNA) was purified by phenol-

438 chloroform extraction; 1-2 µg DNA was used for the construction of the TraDIS sequencing libraries

439 as described previously (37). Amplification of transposon junctions was performed using primer

440 FS108 (NTUH-K2044, B5055 and ATCC43816 libraries) or Tn5tetR_5PCR (RH201207 library). Libraries

441 from the RH201207 strain were sequenced on the Illumina Miseq platform using primer

442 Tn5tetR_5Seq. All other libraries were sequenced on the Illumina HiSeq platform using FS107.

443 Sequencing was performed as described previously (37).

444 **Analysis of TraDIS data.** TraDIS sequencing reads were analyzed using the BioTraDIS pipeline as

445 described previously (37, 68), with the following parameters passed to the bacteria_tradis script: "-v

446 --smalt_y 0.96 --smalt_r -1 -t TAAGAGACAG -mm -1". Reads and insertion sites were assigned to

447 each gene using a custom script (available at https://github.com/francesca-

448 short/tradis_scripts/tradis_insert_sites_FS.py), with reads mapping to the 3' 10 % of the gene

449   ignored. Output samples following treatment with serum or heat-inactivated serum were compared

450   to the input sample, and to each other, using the tradis_comparison.R script without filtering. Hits

451   were defined as those genes with log2FC <-1 or log2FC > 1, q-value < 0.005. Values reported in the

452   manuscript are for serum compared to heat-inactivated serum. A previously generated

453   pangenome(35) from a global collection of 265 *K. pneumoniae* strains(59) was used to identify

454   orthologs between strains and to classify genes as belonging to the *K. pneumoniae* core or accessory

455   genome. Where needed, pathway information on specific genes was extracted from Biocyc(47).

456   **Quantification of capsule.** Capsule production was measured using an assay for uronic acids as

457   described previously (69). Overnight cultures of *K. pneumoniae* were grown in LB at 37 °C and 500 µl

458   aliquots were used directly in the assay. To examine cell-attached capsule, the 500 µl culture

459   samples were centrifuged at 8000 g for 2 min and cell pellets were then suspended in 500 µl fresh LB

460   medium prior to uronic acid quantification. A standard curve of glucuronic acid (Sigma-Aldrich) was

461   used to calculate uronic acid concentrations.

462   **Serum survival assays.** Bacteria were grown overnight in LB, subcultured 1:100 in fresh LB medium,

463   and grown to late exponential phase (OD_{600} = 1). Cultures were then washed once in PBS and diluted

464   1:100 in sterile phosphate-buffered saline; 50 µl diluted culture was added to 100 µl pre-warmed

465   human serum (Sigma) and incubated at 37 °C. Samples were taken at set time points, serially diluted

466   and plated for enumeration of viable bacteria.

467   **Hypermucoidy assay.** Overnight cultures of the strains of interest carrying pBAD33-derived Lpp

468   expression plasmids (Table S1) were grown in LB supplemented with 25 µg/ml chloramphenicol, and

469   subcultured for 5 h in LB + 0.1% L-Ara to induce vector expression. Cultures were centrifuged at 1000

470   g for 5 min, and hypermucoidy expressed as a ratio of OD_{600} of the supernatant / OD_{600} of the

471   original culture.

472   **Construction of mutants.** Clean single-gene deletion mutants in *K. pneumoniae* were constructed as

473   described (35) using pKNG101Tc-derived allelic exchange vectors introduced by conjugation with *E.*

474   *coli* β2163 as donor strain. Details of the plasmids and oligonucleotides used in mutant construction

475   are in Table S1. Defined transposon insertion mutants of ATCC43816 and RH201207 were isolated by

476   subjecting the relevant TraDIS library to two rounds of density-gradient centrifugation (70). The non-

477   capsulated fraction was grown as single colonies and mutant locations identified by random-primed

478   PCR as described (71) using primers FS57-FS60 together with FS108-109 for ATCC43816 and FS346-

479   347 for RH201207 (Table S1). Complementation plasmids were constructed using the primers listed

480   in Table S1 and introduced by electroporation.

481   **Detection of surface-located C' components.** Early mid-logarithmic-phase LB cultures (1ml) were

482   washed in gelatin-veronal-buffered saline containing Mg^{2+} and Ca^{2+} (pH 7.35) (GVB^{2+}), and incubated

483   in 66% prewarmed (37°C) pooled human serum (MP Biomedicals) for 15, 30, 60, 120 and 180 min

484   (1). Prewarmed, heat-inactivated (56°C; 30 min) human pooled serum served to set T0. Human C3-

485   deficient and C5-deficient serum (Sigma) were used as negative controls. For flow cytometric

486   staining, after incubation the mixtures were washed in PBS and approximately $1x10^6$ cells were

487   stained. C3b binding was detected with a mouse monoclonal APC anti-C3b/iC3b antibody

488   (Biolegend) (4µl per 10^6 cells) and C5b-9 formation was detected by indirectly staining cells with

489   8µg/ml mouse anti-C5b-9 antibody [aE11] (abcam) as primary antibody and 2.5µg/ml Alexa

490   Fluor®488 goat anti-mouse IgG H&L (abcam) as secondary antibody. After 20 min incubation at RT,

491   mixtures were washed and suspended in 200 µl PBS. Samples were acquired using a MACSQuant®

492   instrument (Miltenyi Biotec) within 60 min. Approximately 40,000 cell events were collected. Flow

493   cytometry data analysis was carried out using FlowJo 10 Software. Graphpad 7.05 software was used

494   for graph design and statistical analysis.

495   For microscopy, samples of early mid-logarithmic-phase LB cultures (equivalent to 1ml of OD_{600} of

496   0.5) were washed in GVB^{2+}, and incubated with serum for 0, 5 or 15 min.Cells were then washed

497   with PBS, separated into two aliquots and stained with either 10 µg/ml mouse monoclonal APC anti-

498   C3b/iC3b antibody (Biolegend) or 10 µg/ml mouse anti-C5b-9 antibody [aE11] (abcam) followed by

499   10µg/ml Alexa Fluor®488 goat anti-mouse IgG H&L (abcam) for 10min at RT. Cells were washed with

500   PBS following each staining step, resuspended in PBS and mounted on 1% PBS agarose pads for

501 imaging. Highly inclined and laminated optical sheet (HILO) microscopy was performed using the

502 Nanoimager S MarkII from ONI (Oxford Nanoimaging) equipped with lasers 473nm/300mW (10%),

503 640nm/300mW (7%), dual emission channel split at 560nm, 100x oil-immersion objective (Olympus,

504 numerical aperture (NA) 1.49) and an ORCA-Flash4.0 V3 CMOS camera (Hamamatsu). Images were

505 acquired at an illumination angle of 51° with 100ms exposures for >40 frames and processed using

506 FIJI software (72). In brief, transillumination images were generated as an average of 10 frames

507 (total of 1sec exposure) while fluorescence images were processed by averaging 40 images (total of

508 4sec exposure). Brightness and contrast of images in Figs 6 & 7 are normalised.

509 **Measurement of cytoplasmic marker release by B5055 Δ*rfaH***

510 Bacteria containing pFLS21 (Table S1), a pDiGc (73) derivative which expresses GFP from the

511 constitutive *rpsM* promoter, were grown to early log-phase in LB medium, and washed once in PBS.

512 250 µl undiluted cell suspension was combined with 500 µl serum or heat-inactivated serum and

513 incubated at 37 °C. The total GFP fluorescence of a 100 µl sample, and the fluorescence of 100 µl of

514 supernatant following centrifugation at 8000g for 2 min, was measured in a Pherastar fluorimeter at

515 set time points following incubation. Values were calculated as a percentage supernatant

516 fluorescence intensity/total fluorescence intensity, with background signal from 66% human serum

517 with PBS subtracted.

518 **Statistical analysis**

519 TraDIS comparisons were conducted using EdgeR as implemented in the BioTraDIS pipeline, for

520 which the statistical approaches have been described in detail. The Benjamini-Hochberg correction

521 for multiple testing was applied.

522 All quantitative experiments were performed in biological triplicate, with the exception of those

523 shown in Fig S2B (n = 2, 7 technical replicates) and Fig S4B (n = 2). All graphs show mean ± 1SD, and

524 statistical significance is indicated by *p<0.05, **p<0.01, ***p<0.001, ****p<0.0001 throughout.

525 Serum survival data were compared between bacterial strains by two-factor repeated measures

526 ANOVA on $\log_{10}$-transformed bacterial viable counts with Huyhn and Feldt correction. Where the

527   ANOVA indicated a significant time*strain interaction, viability at t = 180 was compared by one-way

528   ANOVA with Dunnett's test for multiple comparisons. Uronic acid quantification and hypermucoidy

529   data were compared between strains by one-way ANOVA on untransformed data followed by

530   Dunnett's post-hoc test to compare multiple strains to a single reference, or the Tukey-Kramer test

531   for all-against-all comparisons. Complement binding time series data were tested for significance by

532   two-factor repeated measures ANOVA on untransformed data, followed by Fisher's protected LSD

533   test to compare mutant to wild-type at individual time points.

534   **DATA AVAILABILITY**

535   The TraDIS sequencing data generated for this study has been deposited in the European Nucleotide

536   Archive (ENA) under project PRJEB20200. Sample-wise accession numbers are provided in Table S2.

546

547   **REFERENCES**

548

549   1.   Moradigaravand D, Martin V, Peacock SJ, Parkhill J. 2017. Evolution and Epidemiology of

550   Multidrug-Resistant *Klebsiella pneumoniae* in the United Kingdom and Ireland. MBio

551   8:e01976-16.

552   2.   Wyres KL, Holt KE. 2018. *Klebsiella pneumoniae* as a key trafficker of drug resistance genes

553   from environmental to clinically important bacteria. Curr Opin Microbiol.45:131-139

554   3.   Bialek-Davenet S, Criscuolo A, Ailloud F, Passet V, Jones L, Delannoy-Vieillard AS, Garin B,

555   Hello S Le, Arlet G, Nicolas-Chanoine MH, Decré D, Brisse S. 2014. Genomic Definition of

556   Hypervirulent and Multidrug-Resistant *Klebsiella pneumoniae* Clonal Groups. Emerg Infect Dis

557   20:1812–1820.

558   4.   Podschun R, Ullmann U. 1998. *Klebsiella* spp. as nosocomial pathogens: epidemiology,

559   taxonomy, typing methods, and pathogenicity factors. Clin Microbiol Rev 11:589–603.

560   5.   Russo TA, Marr CM. 2019. Hypervirulent *Klebsiella pneumoniae*. Clin Microbiol Rev

561   32:e00001-19.

562   6.   Lam MMC, Wyres KL, Duchêne S, Wick RR, Judd LM, Gan Y-H, Hoh C-H, Archuleta S, Molton

563   JS, Kalimuddin S, Koh TH, Passet V, Brisse S, Holt KE. 2018. Population genomics of

564   hypervirulent *Klebsiella pneumoniae* clonal-group 23 reveals early emergence and rapid

565   global dissemination. Nat Commun 9:2703.

566   7.   Gu D, Dong N, Zheng Z, Lin D, Huang M, Wang L, Chan EW-C, Shu L, Yu J, Zhang R, Chen S.

567   2018. A fatal outbreak of ST11 carbapenem-resistant hypervirulent *Klebsiella pneumoniae* in

568   a Chinese hospital: a molecular epidemiological study. Lancet Infect Dis 18:37–46.

569   8.   Bengoechea JA, Pessoa JS. 2018. *Klebsiella pneumoniae* infection biology: living to counteract

570   host defences. FEMS Microbiol Rev 43:123-144.

571   9.   Paczosa MK, Mecsas J. 2016. *Klebsiella pneumoniae*: Going on the Offense with a Strong

572   Defense. Microbiol Mol Biol Rev 80:629–661.

573   10.   Nassif X, Fournier JM, Arondel J, Sansonetti PJ. 1989. Mucoid phenotype of *Klebsiella*

574   *pneumoniae* is a plasmid-encoded virulence factor. Infect Immun 57:546–552.

575   11.   Hsu CR, Lin TL, Chen YC, Chou HC, Wang JT. 2011. The role of *Klebsiella pneumoniae rmpA* in

576   capsular polysaccharide synthesis and virulence revisited. Microbiology 157:3446–3457.

577   12.   Wyres KL, Wick RR, Gorrie C, Jenney A, Follador R, Thomson NR, Holt KE. 2016. Identification

578   of *Klebsiella* capsule synthesis loci from whole genome data. Microb Genomics 2:e000102.

579 13. Trautmann M, Held TK, Cross AS. 2004. O antigen seroepidemiology of *Klebsiella* clinical

580   isolates and implications for immunoprophylaxis of *Klebsiella* infections. Vaccine 22:818–821.

581 14. Martin RM, Bachman MA. 2018. Colonization, Infection, and the Accessory Genome of

582   *Klebsiella pneumoniae*. Front Cell Infect Microbiol 8:1–15.

583 15. Lambris JD, Ricklin D, Geisbrecht B V. 2008. Complement evasion by human pathogens. Nat

584   Rev Microbiol. England.

585 16. DeLeo FR, Kobayashi SD, Porter AR, Freedman B, Dorward DW, Chen L, Kreiswirth BN. 2017.

586   Survival of Carbapenem-Resistant *Klebsiella pneumoniae* Sequence Type 258 in Human

587   Blood. Antimicrob Agents Chemother 61:AAC.02533-16.

588 17. Kobayashi SD, Porter AR, Dorward DW, Brinkworth AJ, Chen L, Kreiswirth BN, DeLeo FR. 2016.

589   Phagocytosis and Killing of Carbapenem-Resistant ST258 *Klebsiella pneumoniae* by Human

590   Neutrophils. J Infect Dis 213:1615–1622.

591 18. Endo Y, Matsushita M, Fujita T. 2011. The role of ficolins in the lectin pathway of innate

592   immunity. Int J Biochem Cell Biol. 43:705-12

593 19. Merle NS, Noe R, Halbwachs-Mecarelli L, Fremeaux-Bacchi V, Roumenina LT. 2015.

594   Complement System Part II: Role in Immunity. Front Immunol 6:257.

595 20. Taylor PW, Kroll HP. 1985. Effect of lethal doses of complement on the functional integrity of

596   target enterobacteria. Curr Top Microbiol Immunol 121:135–158.

597 21. Wang Y, Bjes ES, Esser AF. 2000. Molecular aspects of complement-mediated bacterial killing.

598   Periplasmic conversion of C9 from a protoxin to a toxin. J Biol Chem 275:4687–4692.

599 22. Taylor PW. 1992. Complement-mediated killing of susceptible gram-negative bacteria: an

600   elusive mechanism. Exp Clin Immunogenet 9:48–56.

601 23. Alberti S, Marques G, Camprubi S, Merino S, Tomas JM, Vivanco F, Benedi VJ. 1993. C1q

602   binding and activation of the complement classical pathway by *Klebsiella pneumoniae* outer

603   membrane proteins. Infect Immun 61:852–860.

604 24. Alberti S, Alvarez D, Merino S, Casado MT, Vivanco F, Tomas JM, Benedi VJ. 1996. Analysis of

605   complement C3 deposition and degradation on *Klebsiella pneumoniae*. Infect Immun

606   64:4726–4732.

607 25. DeLeo FR, Kobayashi SD, Porter AR, Freedman B, Dorward DW, Chen L, Kreiswirth BN. 2017.

608   Survival of carbapenem-resistant ST258 *Klebsiella pneumoniae* in human blood. Antimicrob

609   Agents Chemother AAC.02533-16.

610 26. Jensen TS, Opstrup KV, Christiansen G, Rasmussen PV, Thomsen ME, Justesen DL,

611   Schønheyder HC, Lausen M, Birkelund S. 2020. Complement mediated *Klebsiella pneumoniae*

612   capsule changes. Microbes Infect 22:19–30.

613 27. Doorduijn DJ, Rooijakkers SHM, van Schaik W, Bardoel BW. 2016. Complement resistance

614   mechanisms of *Klebsiella pneumoniae*. Immunobiology 221:1102–1109.

615 28. Loraine J, Heinz E, De Sousa Almeida J, Milevskyy O, Voravuthikunchai SP, Srimanote P,

616   Kiratisin P, Thomson NR, Taylor PW. 2018. Complement Susceptibility in Relation to Genome

617   Sequence of Recent *Klebsiella pneumoniae* Isolates from Thai Hospitals. mSphere 3:1–15.

618 29. Diago-Navarro E, Motley MP, Ruiz-Perez G, Yu W, Austin J, Seco BMS, Xiao G, Chikhalya A,

619   Seeberger PH, Fries BC. 2018. Novel, Broadly Reactive Anticapsular Antibodies against

620   Carbapenem-Resistant *Klebsiella pneumoniae* Protect from Infection. MBio 9: e00091-18

621 30. Kobayashi SD, Porter AR, Freedman B, Pandey R, Chen L, Kreiswirth BN, DeLeo FR. 2018.

622   Antibody-mediated killing of carbapenem-resistant ST258 *Klebsiella pneumoniae* by human

623   neutrophils. MBio 9:e00297-18

624 31. Namikawa H, Oinuma KI, Sakiyama A, Tsubouchi T, Tahara YO, Yamada K, Niki M, Takemoto Y,

625   Miyata M, Kaneko Y, Shuto T, Kakeya H. 2019. Discovery of anti-mucoviscous activity of

626   rifampicin and its potential as a candidate antivirulence agent against hypervirulent *Klebsiella*

627   *pneumoniae*. Int J Antimicrob Agents.

628 32. Wu KM, Li LH, Yan JJ, Tsao N, Liao TL, Tsai HC, Fung CP, Chen HJ, Liu YM, Wang JT, Fang CT,

629   Chang SC, Shu HY, Liu TT, Chen YT, Shiau YR, Lauderdale TL, Su IJ, Kirby R, Tsai SF. 2009.

630   Genome sequencing and comparative analysis of *Klebsiella pneumoniae* NTUH-K2044, a

631   strain causing liver abscess and meningitis. J Bacteriol 191:4492–4501.

632   33. Broberg CA, Wu W, Cavalcoli JD, Miller VL, Bachman MA. 2014. Complete genome sequence

633   of *Klebsiella pneumoniae* strain ATCC 43816 KPPR1, a rifampin-resistant mutant commonly

634   used in animal, genetic, and molecular biology studies. Genome Announc 2:e00924-14-

635   e00924-14.

636   34. Jana B, Cain AK, Doerrler WT, Boinett CJ, Fookes MC, Parkhill J, Guardabassi L. 2017. The

637   secondary resistome of multidrug-resistant *Klebsiella pneumoniae*. Sci Rep 7:42483.

638   35. Dorman MJ, Feltwell T, Goulding DA, Parkhill J, Short FL. 2018. The capsule regulatory

639   network of *Klebsiella pneumoniae* defined by density-traDISort. MBio 9.

640   36. Phan MD, Peters KM, Sarkar S, Lukowski SW, Allsopp LP, Moriel DG, Achard MES, Totsika M,

641   Marshall VM, Upton M, Beatson SA, Schembri MA. 2013. The serum resistome of a globally

642   disseminated multidrug resistant uropathogenic *Escherichia coli* clone. PLoS Genet 9:

643   e1003834.

644   37. Barquist L, Mayho M, Cummins C, Cain AK, Boinett CJ, Page AJ, Langridge GC, Quail MA,

645   Keane JA, Parkhill J. 2016. The TraDIS toolkit: Sequencing and analysis for dense transposon

646   mutant libraries. Bioinformatics 32:1109–1111.

647   38. Tan YH, Chen Y, Chu WHW, Sham LT, Gan YH. 2020. Cell envelope defects of different

648   capsule-null mutants in K1 hypervirulent *Klebsiella pneumoniae* can affect bacterial

649   pathogenesis. Mol Microbiol 2020;00:1–17

650   39. Cai R, Wang G, Le S, Wu M, Cheng M, Guo Z, Ji Y, Xi H, Zhao C, Wang X, Xue Y, Wang Z, Zhang

651   H, Fu Y, Sun C, Feng X, Lei L, Yang Y, Ur Rahman S, Liu X, Han W, Gu J. 2019. Three capsular

652   polysaccharide synthesis-related glucosyltransferases, GT-1, GT-2 and WcaJ, are associated

653   with virulence and phage sensitivity of *Klebsiella pneumoniae.* Front Microbiol 10:1–14.

654   40. Bachman MA, Breen P, Deornellas V, Mu Q, Zhao L, Wu W, Cavalcoli JD. 2015. Genome-Wide

655   Identification of *Klebsiella pneumoniae* fitness genes during lung infection. MBio 6:e00775-

656   15.

657 41. Bailey MJA, Hughes C, Koronakis V. 1997. RfaH and the *ops* element, components of a novel

658   system controlling bacterial transcription elongation. Mol Microbiol 26:845–851.

659 42. Walker KA, Miner TA, Palacios M, Trzilova D, Frederick DR, Broberg CA, Sepúlveda VE, Quinn

660   JD, Miller VL. 2019. A *Klebsiella pneumoniae* Regulatory Mutant Has Reduced Capsule

661   Expression but Retains Hypermucoviscosity. MBio 10:e00089-19.

662 43. Wall E, Majdalani N, Gottesman S. 2018. The Complex Rcs Regulatory Cascade. Annu Rev

663   Microbiol 72:111-139.

664 44. Miajlovic H, Smith SG. 2014. Bacterial self-defence: How *Escherichia coli* evades serum killing.

665   FEMS Microbiol Lett 354:1–9.

666 45. Taylor PW, Robinson MK. 1980. Determinants that increase the serum resistance of

667   *Escherichia coli*. Infect Immun 29:278–280.

668 46. Llobet E, Martínez-Moliner V, Moranta D, Dahlström KM, Regueiro VV, Tomás A, Cano V,

669   Pérez-Gutiérrez C, Frank CG, Fernández-Carrasco H, Insua JL, Salminen TA, Garmendia J,

670   Bengoechea JA. 2015. Deciphering tissue-induced *Klebsiella pneumoniae* lipid A structure.

671   Proc Natl Acad Sci 112:E6369–E6378.

672 47. Karp PD, Billington R, Caspi R, Fulcher CA, Latendresse M, Kothari A, Keseler IM,

673   Krummenacker M, Midford PE, Ong Q, Ong WK, Paley SM, Subhraveti P. 2018. The BioCyc

674   collection of microbial genomes and metabolic pathways. Brief Bioinform 20:1085–1093.

675 48. Hsieh P-F, Liu J-Y, Pan Y-J, Wu M-C, Lin T-L, Huang Y-T Te, Wang J-T. 2013. *Klebsiella*

676   *pneumoniae* peptidoglycan-associated lipoprotein and murein lipoprotein contribute to

677   serum resistance, antiphagocytosis, and proinflammatory cytokine stimulation. J Infect Dis

678   208:1580–1589.

679 49. Asmar AT, Collet JF. 2018. Lpp, the Braun lipoprotein, turns 50—major achievements and

680   remaining issues. FEMS Microbiol Lett 365:1–8.

681 50. Diao J, Bouwman C, Yan D, Kang J, Katakam AK, Liu P, Pantua H, Abbas AR, Nickerson NN,

682   Austin C, Reichelt M, Sandoval W, Xu M, Whitfield C, Kapadia SB. 2017. Peptidoglycan

683   association of murein lipoprotein is required for KpsD-dependent group 2 capsular

684   polysaccharide expression and serum resistance in a uropathogenic *Escherichia coli* isolate.

685   MBio 8:e00603-17.

686   51.   Gatzeva-Topalova PZ, May AP, Sousa MC. 2005. Structure and mechanism of ArnA:

687   Conformational change implies ordered dehydrogenase mechanism in key enzyme for

688   polymyxin resistance. Structure 13:929–942.

689   52.   Matsuura M. 2013. Structural Modifications of Bacterial Lipopolysaccharide that Facilitate

690   Gram-Negative Bacteria Evasion of Host Innate Immunity. Front Immunol 4:109.

691   53.   Leskinen K, Varjosalo M, Li Z, Li CM, Skurnik M. 2015. Expression of the *Yersinia enterocolitica*

692   O:3 LPS O-antigen and outer core gene clusters is RfaH-dependent. Microbiol 161:1282–1294.

693   54.   Farewell A, Brazas R, Davie E, Mason J, Rothfield LI. 1991. Suppression of the abnormal

694   phenotype of Salmonella typhimurium *rfaH* mutants by mutations in the gene for

695   transcription termination factor Rho. J Bacteriol 173:5188–5193.

696   55.   van Opijnen T, Dedrick S, Bento J. 2016. Strain Dependent Genetic Networks for Antibiotic-

697   Sensitivity in a Bacterial Pathogen with a Large Pan-Genome. PLOS Pathog 12:e1005869.

698   56.   Barquist L, Langridge GC, Turner DJ, Phan MD, Turner AK, Bateman A, Parkhill J, Wain J,

699   Gardner PP. 2013. A comparison of dense transposon insertion libraries in the *Salmonella*

700   serovars Typhi and Typhimurium. Nucleic Acids Res 41:4549–4564.

701   57.   Poulsen BE, Yang R, Clatworthy AE, White T, Osmulski SJ, Li L, Penaranda C, Lander ES,

702   Shoresh N, Hung DT. 2019. Defining the core essential genome of *Pseudomonas aeruginosa*.

703   Proc Natl Acad Sci 116:10072–10080.

704   58.   Carey AF, Rock JM, Krieger I V, Chase MR, Fernandez-Suarez M, Gagneux S, Sacchettini JC,

705   Ioerger TR, Fortune SM. 2018. TnSeq of *Mycobacterium tuberculosis* clinical isolates reveals

706   strain-specific antibiotic liabilities. PLOS Pathog 14:e1006939.

707   59.   Holt KE, Wertheim H, Zadoks RN, Baker S, Whitehouse CA, Dance D, Jenney A, Connor TR, Hsu

708   LY, Severin J, Brisse S, Cao H, Wilksch J, Gorrie C, Schultz MB, Edwards DJ, Van Nguyen K,

709   Nguyen TV, Dao TT, Mensink M, Le Minh V, Nhu NTK, Schultsz C, Kuntaman K, Newton PN,

710   Moore CE, Strugnell RA, Thomson NR. 2015. Genomic analysis of diversity, population

711   structure, virulence, and antimicrobial resistance in *Klebsiella pneumoniae*, an urgent threat

712   to public health. Proc Natl Acad Sci 112:E3574–E3581.

713 60. Mushtaq N, Redpath MB, Luzio JP, Taylor PW. 2004. Prevention and cure of systemic

714   *Escherichia coli* K1 infection by modification of the bacterial phenotype. Antimicrob Agents

715   Chemother 48:1503–1508.

716 61. Majkowska-Skrobek G, Latka A, Berisio R, Squeglia F, Maciejewska B, Briers Y, Drulis-Kawa Z.

717   2018. Phage-borne depolymerases decrease *Klebsiella pneumoniae* resistance to innate

718   defense mechanisms. Front Microbiol 9:1–12.

719 62. Liu Y, Leung SSY, Huang Y, Guo Y, Jiang N, Li P, Chen J, Wang R, Bai C, Mi Z, Gao Z. 2020.

720   Identification of Two Depolymerases From Phage IME205 and Their Antivirulent Functions on

721   K47 Capsule of *Klebsiella pneumoniae*. Front Microbiol 11:1–11.

722 63. Pan YJ, Lin TL, Chen YY, Lai PH, Tsai YT, Hsu CR, Hsieh PF, Lin YT, Wang JT. 2019. Identification

723   of three podoviruses infecting *Klebsiella* encoding capsule depolymerases that digest specific

724   capsular types. Microb Biotechnol 12:472–486.

725 64. Lin TL, Hsieh PF, Huang YT, Lee WC, Tsai YT, Su PA, Pan YJ, Hsu CR, Wu MC, Wang JT. 2014.

726   Isolation of a bacteriophage and its depolymerase specific for K1 capsule of *Klebsiella*

727   *pneumoniae:* Implication in typing and treatment. J Infect Dis 210:1734–1744.

728 65. Wang C, Li P, Niu W, Yuan X, Liu H, Huang Y, An X, Fan H, Zhangxiang L, Mi L, Zheng J, Liu Y,

729   Tong Y, Mi Z, Bai C. 2019. Protective and therapeutic application of the depolymerase derived

730   from a novel KN1 genotype of *Klebsiella pneumoniae* bacteriophage in mice. Res Microbiol

731   170:156–164.

732 66. Pan YJ, Lin TL, Lin YT, Su PA, Chen CT, Hsieh PF, Hsu CR, Chen CC, Hsieh YC, Wang JT. 2015.

733   Identification of capsular types in carbapenem-resistant *Klebsiella pneumoniae* strains by wzc

734   sequencing and implications for capsule depolymerase treatment. Antimicrob Agents

735   Chemother 59:1038–1047.

736   67.   Taylor PW. 1985. Measurement of the bactericidal action of serum, p. 445–456. *In* Virulence

737   of Escherichia coli. M. Sussman Academic Press, New York.

738   68.   Langridge GC, Phan MD, Turner DJ, Perkins TT, Parts L, Haase J, Charles I, Maskell DJ, Peters

739   SE, Dougan G, Wain J, Parkhill J, Turner AK. 2009. Simultaneous assay of every *Salmonella*

740   Typhi gene using one million transposon mutants. Genome Res 19:2308–2316.

741   69.   Favre-Bonte S, Joly B, Forestier C. 1999. Consequences of reduction of *Klebsiella pneumoniae*

742   capsule expression on interactions of this bacterium with epithelial cells. Infect Immun

743   67:554–561.

744   70.   Feltwell T, Dorman MJ, Goulding DA, Parkhill J, Short FL. 2019. Separating Bacteria by Capsule

745   Amount Using a Discontinuous Density Gradient. J Vis Exp e58679.

746   71.   Fineran PC, Everson L, Slater H, Salmond GPC. 2005. A GntR family transcriptional regulator

747   (PigT) controls gluconate-mediated repression and defines a new, independent pathway for

748   regulation of the tripyrrole antibiotic, prodigiosin, in *Serratia*. Microbiology 151:3833–3845.

749   72.   Schindelin J, Arganda-Carreras I, Frise E, Kaynig V, Longair M, Pietzsch T, Preibisch S, Rueden

750   C, Saalfeld S, Schmid B, Tinevez J, White DJ, Hartenstein V, Eliceiri K, Tomancak P, Cardona A.

751   2019. Fiji: an open-source platform for biological-image analysis. Nat Methods 9:676-82.

752   73.   Helaine S, Thompson JA, Watson KG, Liu M, Boyle C, Holden DW. 2010. Dynamics of

753   intracellular bacterial replication at the single cell level. Proc Natl Acad Sci 107:3746–3751.

754

755

756 **Figures**

757 **Fig 1. Characteristics of *K. pneumoniae* strains used in this study** (A) Schematic of the four strains

758 used in this study, with sequence type, O-antigen and capsule types indicated. (B) Quantification of

759 capsular uronic acids in four *K. pneumoniae* strains (n = 3). Statistically significant differences

760 between strains were determined by one-way ANOVA (overall p<0.0001) followed by Tukey's HSD

761 test, **p<0.01, ***p<0.001, ****p<0.0001. Overall significance is indicated above chart. (C)

762 Resistance of the four *K. pneumoniae* strains to killing by pooled human serum (n = 3). Strains were

763 compared by two-factor repeated measures ANOVA (overall p<0.0001), and Tukey's HSD test at

764 t=180 showed RH201207 to be significantly different from each of the other three strains,

765 ***p<0.001.

766 **Fig 2. Genes contributing to serum resistance in four *K. pneumoniae* strains** (A) Venn diagram

767 showing the overlap in genes involved in serum survival in each strain. Hit genes are defined as

768 those with a log2FC < -1 or >1, q-value < 0.005. Full results are in Table S3 and TraDIS hits in Table S4.

769 (B) Abundance of transposon mutants following serum treatment, relative to treatment with heat-

770 inactivated serum. Volcano plots of log2-fold change and log10 p-value are shown for each strain.

771 Genes with very low read counts in any condition are excluded. Key resistance factors (capsule, O-

772 antigen, Lpp, RfaH and ArnDEF) are indicated by colour.

773 **Fig 3. Strain specificity of complement resistance in *K. pneumoniae*** Discontinuous heatmap of

774 TraDIS hits for complement resistance. Homologues across different strains were determined by

775 BLASTp (cutoff >90% amino acid identity) in the process of constructing the *K. pneumoniae*

776 pangenome (see materials and methods). Capsule and O-antigen locus types was determined using

777 Kaptive-Web and the corresponding gene names are used. The three genes outside of the capsule

778 and LPS loci that were required for complement resistance in all four strains are indicated in red

779 text. Genes marked "NA" are either absent from that strain, or have been excluded from the

780 comparative analysis due to having very low read counts in any condition. Full details are in Table S3
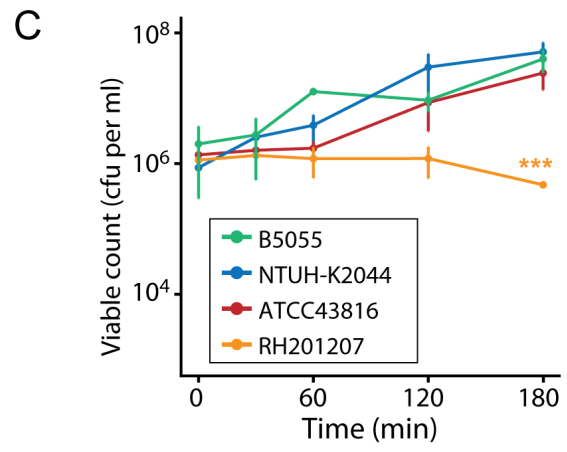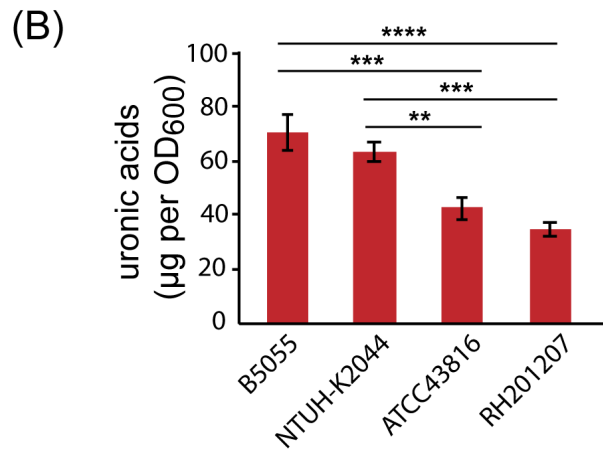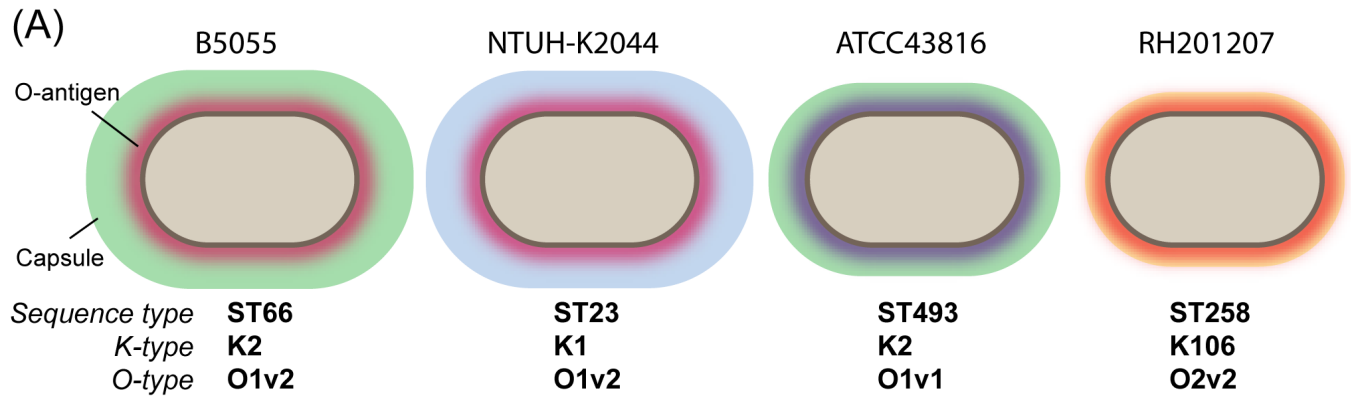
781 and Table S4.

782 **Fig 4. Validation of serum survival defects in Δ*rfaH* and Δ*lpp* mutants** Total bacterial viable count of

783 *K. pneumoniae* strains and key mutants following incubation with 66% pooled normal human serum

784 (see Materials and Methods). The detection limit of the assay is 2x 10^3 viable cells per ml. Overall

785 statistical significance was determined by two-factor repeated measures ANOVA (p<0.0001 for all

786 strains), mutants were compared to wild-type at t=180 by single-factor ANOVA and Dunnett's test at

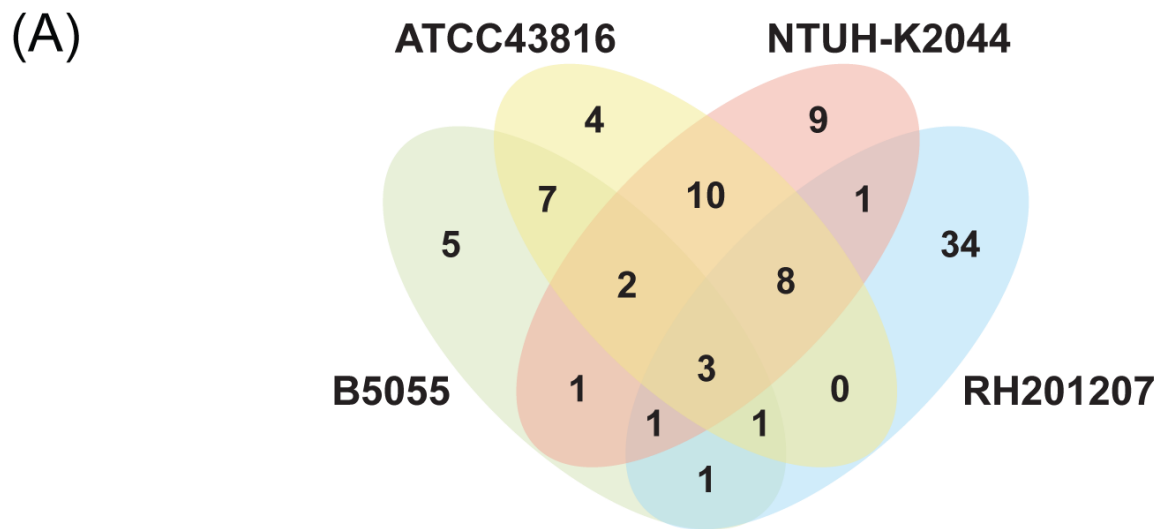787 t=180 (**p<0.01). ATCC43816 WT and mutants n = 5, all other strains n = 3.

788 **Fig 5. Effects of Lpp and RfaH on capsule production and retention** (A) Comparison of total and cell-

789 attached capsule content of wild-type and Δ*lpp* mutants of *K. pneumoniae* ATCC43816, B5055 and

790 NTUH-K2044 (n = 3). Uronic acids were either quantified directly from culture or following a single

791 wash and resuspension in LB (see Materials and Methods), and Δ*lpp* values were normalised to the

792 WT from the same strain and condition. All three strains showed a significant reduction in cell-

793 associated capsule, while total capsule was unchanged or increased (one-way ANOVA relative to WT,

794 *p<0.05 **p<0.01 ***p<0.001). (B) Comparison of capsule production in Δ*rfaH* mutant and

795 complemented mutant strains (n = 3). Overall statistical significance for each strain was determined

796 by one-way ANOVA, Δ*rfaH* mutant and complemented strains were compared to WT by Dunnett's

797 post-hoc test. RH201207 Δ*rfaH* was compared to WT by one-way ANOVA. *p<0.05, **p<0.01. (C)

798 Partial complementation of *K. pneumoniae* Δ*lpp* mutants using an inducible vector (n = 3). The

799 hypermucoidy assay for capsule was performed on stationary-phase, arabinose-induced cultures

800 washed once in PBS. Induction of wild-type Lpp partially restored the hypermucoid phenotype of the

801 NTUH-K2044 and B5055 Δ*lpp* mutants. This effect was not seen with the empty vector, or with an

802 Lpp construct lacking its C-terminal lysine (ΔK78). Overall significance for each strain was determined

803 by one-way ANOVA, followed by Dunnett's post-hoc test to compare each WT or complemented

804 strain to Δ*lpp* + vector. *p<0.05, **p<0.01.

805 **Fig 6. C3b binding to the bacterial cell surface** (A) Flow cytometry-based determination of C3b

806 binding to ATCC43816, B5055, NTUH-K2044, RH201207 and their respective mutants were measured

807 after 15, 30, 60, 120 and 180 min incubation in human pooled serum at 37°C (n = 3). Values were
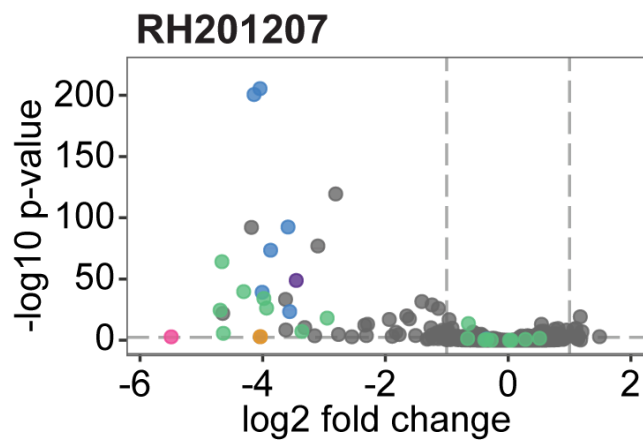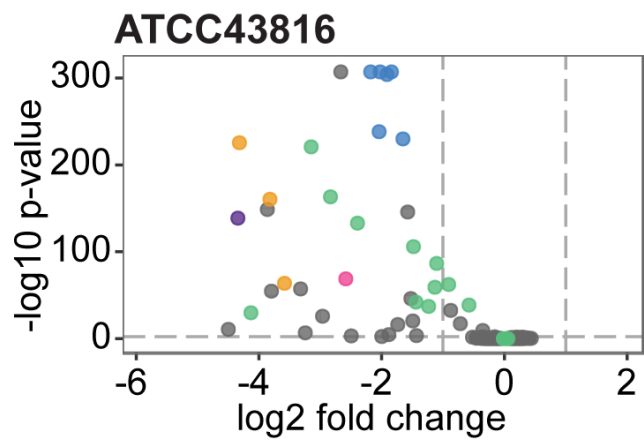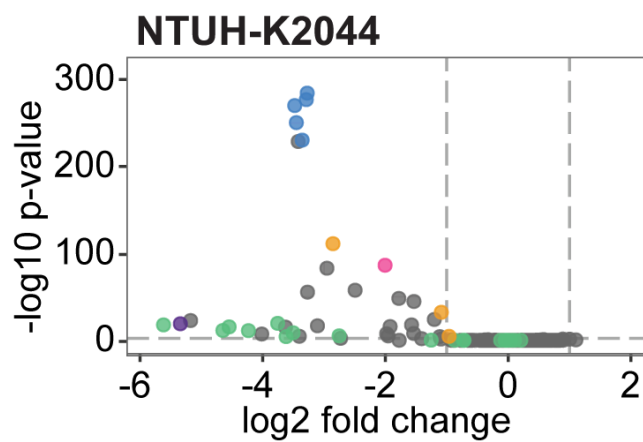
808   converted to A.U., setting T0 to 1. Two-way repeated measures ANOVA with uncorrected Fisher's

809   LSD test revealed: * P ≤ 0.05, ** P ≤ 0.01, ***, P ≤ 0.001; ****, P ≤ 0.0001. For B5055 Δ*rfaH* , data

810   was collected only at the first two time points due to cell lysis detected by release of cytoplasmic

811   fluorescent marker from labelled cells. (B-C) Fluorescence microscopy of 5 min and 15 min serum

812   exposed Δ*rfaH* and WT cells (B) or 15 min serum exposed Δ*lpp* and WT cells (C) following incubation

813   with APC conjugated anti-C3b antibody. Data are representative of three independent experiments.

814   For comparison of binding patterns and intensity, transillumination (left) and fluorescence images

815   (right) are normalised within each panel. Scale bar, 2µm.

816   **Fig 7. C5b-9 binding to the bacterial cell surface** (A) Flow cytometry-based determination of C5b-9

817   formation on ATCC43816, B5055, NTUH-K2044, RH201207 and their respective mutants after 15, 30,

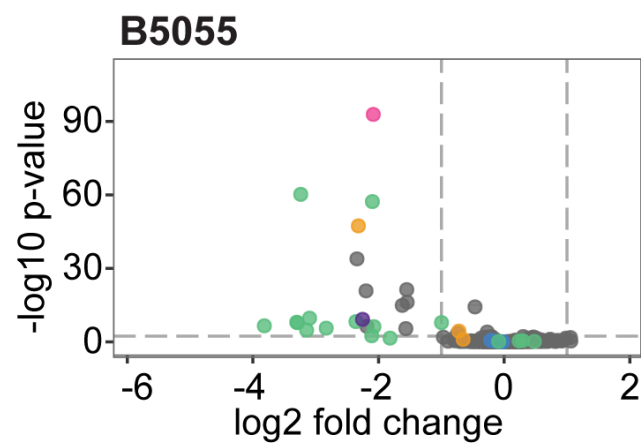818   60, 120 and 180 min incubation in human pooled serum at 37°C (n = 3). Values were converted to

819   A.U., setting T0 to 1. Two-way repeated measures ANOVA with uncorrected Fisher's LSD test

820   revealed: * P ≤ 0.05, ** P ≤ 0.01, ***, P ≤ 0.001; ****, P ≤ 0.0001. For B5055 Δ*rfaH* , data was

821   collected only at the first two time points due to cell lysis detected by release of cytoplasmic

822   fluorescent marker from labelled cells. (B-C) Fluorescence microscopy of 5 min and 15 min serum

823   exposed Δ*rfaH* and WT cells (B) or 15 min serum exposed Δ*lpp* and WT cells (C) following incubation

824   with mouse anti-C5b-9 antibody and AF488 goat anti-mouse IgG. Data are representative of three

825   independent experiments. For comparison of binding patterns and intensity, transillumination (left)

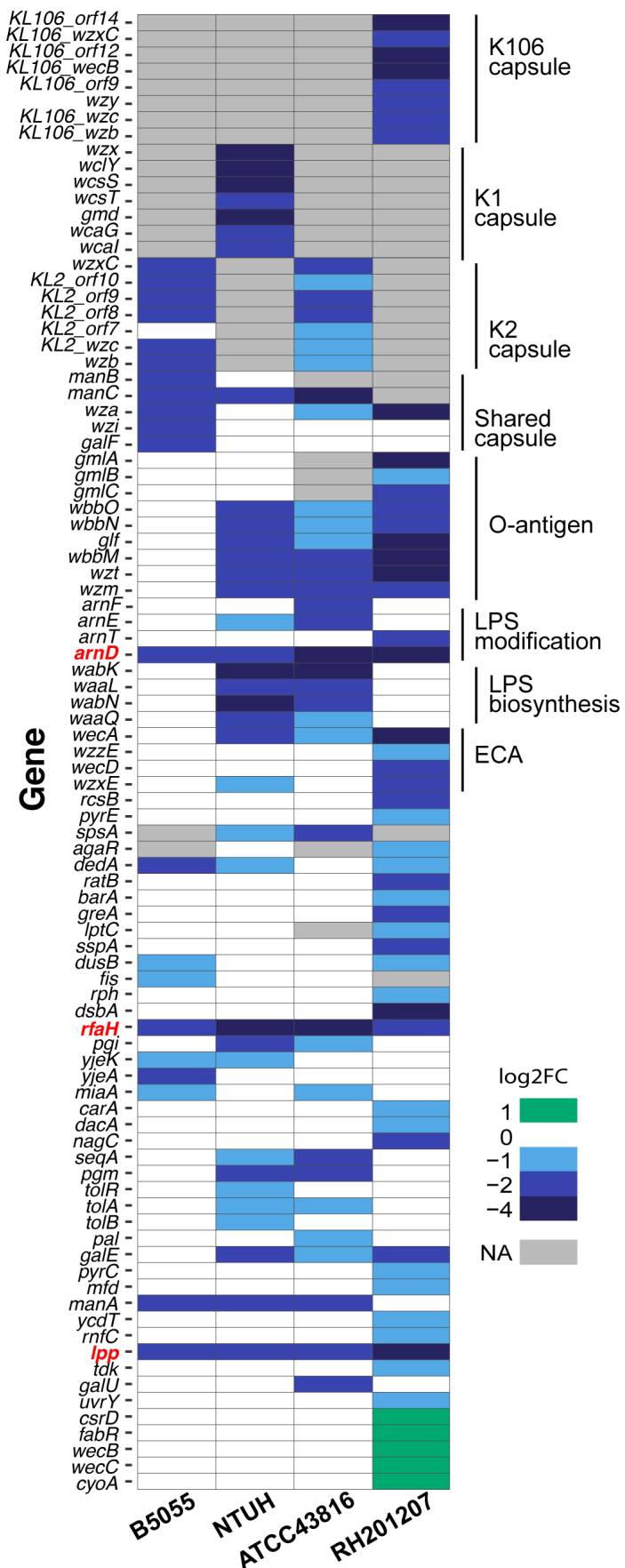826   and fluorescence images (right) are normalised within each panel. Scale bar, 2µm.

(A)

B5055

O-antigen

Capsule

NTUH-K2044

ATCC43816

RH201207

Sequence type	**ST66**	**ST23**	**ST493**	**ST258**
K-type	**K2**	**K1**	**K2**	**K106**
O-type	**O1v2**	**O1v2**	**O1v1**	**O2v2**

(B)

C

(A)

ATCC43816   NTUH-K2044

4   9

7   10   1

5   34

2   8

B5055   RH201207

1   3   0

1   1

1

(B)

Capsule   O-antigen   Lpp   RfaH   ArnDEF   Other

B5055

NTUH-K2044

ATCC43816

RH201207

B5055

NTUH-K2044

ATCC43816

RH201207

Legend: ● WT ● Δ*lpp* ● Δ*rfaH* ● Δ*rfaH* pMJD82

Y-axis: Viable count (cfu per ml)

X-axis: Time (min)

(A)

uronic acids (% relative to WT)

Total capsule (red), Cell-attached capsule (blue)

B5055: WT, Δlpp, WT, Δlpp *
NTUH-K2044: WT, Δlpp, WT, Δlpp ***
ATCC43816: WT, Δlpp *, WT, Δlpp **

(B)

uronic acids (μg per OD600)

B5055: WT, $\Delta rfaH$ **, $\Delta rfaH$ comp ** ($p<0.0001$)
NTUH-K2044: WT, $\Delta rfaH$ **, $\Delta rfaH$ comp ** ($p<0.0001$)
ATCC43816: WT, $\Delta rfaH$ **, $\Delta rfaH$ comp ($p<0.001$)
RH201207: WT, ins-$rfaH$ *

(C)

Hypermucoidy (supernatant OD$_{600}$/ input OD$_{600}$)

B5055: Δlpp + Vector, Δlpp + Lpp *, Δlpp + Lpp $\Delta K78$, WT + Vector ** ($p<0.0001$)
NTUH-K2044: Δlpp + Vector, Δlpp + Lpp **, Δlpp + Lpp $\Delta K78$, WT + Vector ** ($p<0.0001$)

(A)

(B)

(C)

(A)

(B)

(C)